

IL-6 negatively regulates osteoblast differentiation through the SHP2/MEK2 and SHP2/Akt2 pathways in vitro

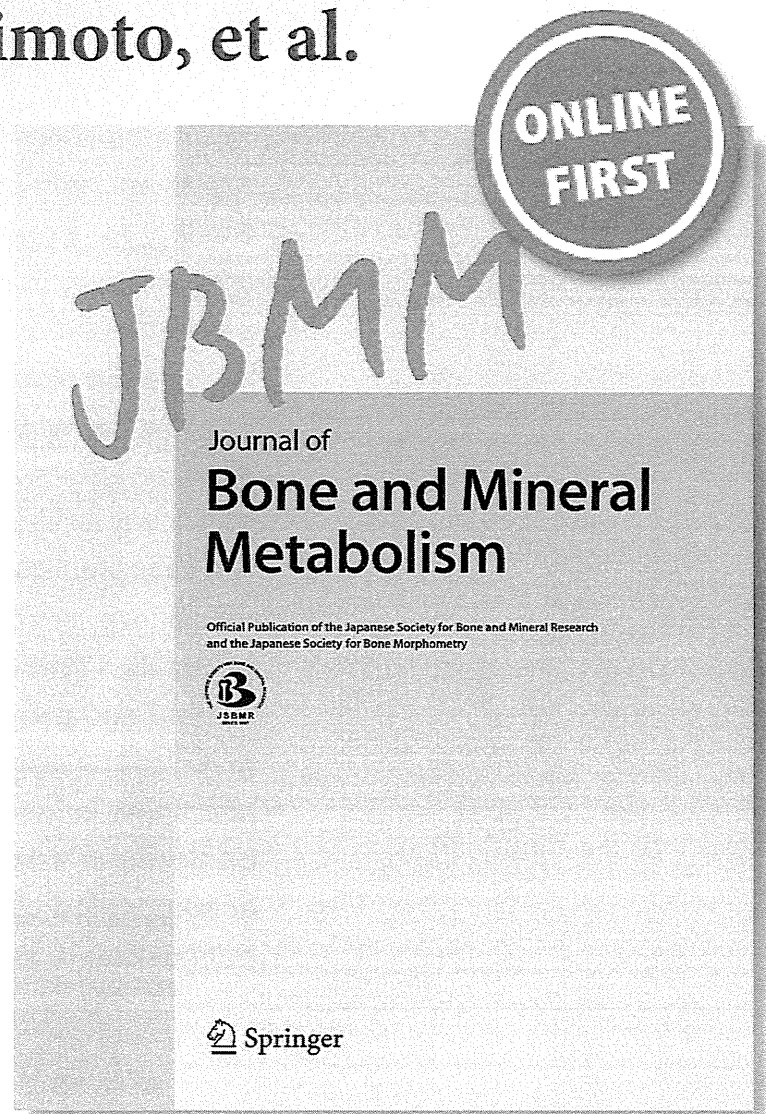
Shoichi Kaneshiro, Kosuke Ebina, Kenrin Shi, Chikahisa Higuchi, Makoto Hirao, Michio Okamoto, Kota Koizumi, Tokimitsu Morimoto, et al.

Journal of Bone and Mineral Metabolism

ISSN 0914-8779

J Bone Miner Metab

DOI 10.1007/s00774-013-0514-1



Your article is protected by copyright and all rights are held exclusively by The Japanese Society for Bone and Mineral Research and Springer Japan. This e-offprint is for personal use only and shall not be self-archived in electronic repositories. If you wish to self-archive your article, please use the accepted manuscript version for posting on your own website. You may further deposit the accepted manuscript version in any repository, provided it is only made publicly available 12 months after official publication or later and provided acknowledgement is given to the original source of publication and a link is inserted to the published article on Springer's website. The link must be accompanied by the following text: "The final publication is available at link.springer.com".

IL-6 negatively regulates osteoblast differentiation through the SHP2/MEK2 and SHP2/Akt2 pathways in vitro

Shoichi Kaneshiro · Kosuke Ebina · Kenrin Shi · Chikahisa Higuchi · Makoto Hirao · Michio Okamoto · Kota Koizumi · Tokimitsu Morimoto · Hideki Yoshikawa · Jun Hashimoto

Received: 13 February 2013 / Accepted: 7 August 2013
© The Japanese Society for Bone and Mineral Research and Springer Japan 2013

Abstract It has been suggested that interleukin-6 (IL-6) plays a key role in the pathogenesis of rheumatoid arthritis (RA), including osteoporosis not only in inflamed joints but also in the whole body. However, previous in vitro studies regarding the effects of IL-6 on osteoblast differentiation are inconsistent. The aim of this study was to examine the effects and signal transduction of IL-6 on osteoblast differentiation in MC3T3-E1 cells and primary murine calvarial osteoblasts. IL-6 and its soluble receptor significantly reduced alkaline phosphatase (ALP) activity, the expression of osteoblastic genes (Runx2, osterix, and osteocalcin), and mineralization in a dose-dependent manner, which indicates negative effects of IL-6 on osteoblast differentiation. Signal transduction studies demonstrated that IL-6 activated not only two major signaling pathways, SHP2/MEK/ERK and JAK/STAT3, but also the SHP2/PI3K/Akt2 signaling pathway. The negative

effect of IL-6 on osteoblast differentiation was restored by inhibition of MEK as well as PI3K, while it was enhanced by inhibition of STAT3. Knockdown of MEK2 and Akt2 transfected with siRNA enhanced ALP activity and gene expression of Runx2. These results indicate that IL-6 negatively regulates osteoblast differentiation through SHP2/MEK2/ERK and SHP2/PI3K/Akt2 pathways, while affecting it positively through JAK/STAT3. Inhibition of MEK2 and Akt2 signaling in osteoblasts might be of potential use in the treatment of osteoporosis in RA.

Keywords Interleukin-6 · Osteoblast differentiation · MEK2 · Akt2 · Signaling pathway

Introduction

Inflammation-mediated bone loss is a major feature of various bone diseases, including rheumatoid arthritis (RA). Interleukin-6 (IL-6) contributes to the development of arthritis and is present at high concentrations in the serum and synovial fluid of patients with RA [1–4]. Soluble IL-6 receptor (sIL-6R) is also elevated in the serum and synovial fluid of RA patients [5, 6], and IL-6 exerts its action by binding either to its membrane-bound receptor (mIL-6R) or to sIL-6R. Moreover, IL-6 is closely associated with the expression of receptor activator of NF- κ B ligand (RANKL) in osteoblasts [7]. That is to say, IL-6 acts indirectly on osteoclastogenesis by stimulating the release of RANKL by cells within bone tissues such as osteoblasts [8]. It can unquestionably be said that IL-6 plays a major role in the pathogenesis of RA [9–12], including osteoporosis not only in inflamed joints but also in the whole body.

There have been several studies on the effect of IL-6 on bone turnover in animal models. In IL-6 knock-out mice,

Electronic supplementary material The online version of this article (doi:10.1007/s00774-013-0514-1) contains supplementary material, which is available to authorized users.

S. Kaneshiro · K. Ebina (✉) · K. Shi · C. Higuchi · M. Okamoto · K. Koizumi · T. Morimoto · H. Yoshikawa
Department of Orthopaedic Surgery, Graduate School of Medicine, Osaka University, 2-2 Yamadaoka, Suita, Osaka 565-0871, Japan
e-mail: k-ebina@umin.ac.jp

M. Hirao
Department of Orthopaedic Surgery, Osaka Minami Medical Center, National Hospital Organization, 2-1 Kidohigashi, Kawachinagano, Osaka 586-8521, Japan

J. Hashimoto
Department of Rheumatology, Osaka Minami Medical Center, National Hospital Organization, 2-1 Kidohigashi, Kawachinagano, Osaka 586-8521, Japan

microstructure abnormalities in cortical bones and delayed fracture healing were observed [13, 14], in spite of the evident normal phenotype [15]. Also, bone loss after estrogen depletion was mitigated in IL-6-deficient mice, while a high level of IL-6 and bone loss are seen in wild-type mice [13]. Moreover, IL-6-overexpressed-transgenic mice develop osteopenia and defective ossification, in which the activity of mature osteoblasts is significantly decreased [16]. All these findings, together with studies on human RA patients [17, 18], indicate that IL-6 plays a major role in bone turnover and is an important regulator of bone homeostasis.

Recently, several biological agents have been introduced for the treatment of RA and have demonstrated not only potent anti-inflammatory effects but also inhibitory effects on joint destruction. Among these biological agents, tocilizumab, an anti-IL-6 receptor antibody, has been reported to increase serum bone formation markers in RA patients [19], suggesting that IL-6 has a negative effect on osteoblast differentiation. However, previous reports regarding the effects of IL-6 on osteoblast differentiation *in vitro* have been inconsistent [20]. IL-6 has been shown to decrease the expression of differentiation markers in osteoblasts [21, 22] and to inhibit bone formation [23], while it has been shown to induce osteoblast differentiation [24, 25].

Binding of IL-6 with sIL-6R or mIL-6R leads to subsequent homodimerization of the signal-transducing molecule gp130, followed by activation of two major intracellular signaling pathways, Janus protein tyrosine kinase (JAK)/signal transducer and activator of transcription factors (STAT) 3, or Src-homology domain 2 containing protein-tyrosine phosphatase (SHP2)/mitogen-activated protein kinase-extracellular signal-regulated kinase kinase (MEK)/mitogen-activated protein kinase (MAPK), also called extracellular signal-regulated kinase (ERK) [26]. There have been many reports in which the effects of IL-6 on JAK/STAT3 and SHP2/ERK signal transduction pathways have been studied in osteoblasts, though it is still controversial whether differentiation is enhanced by IL-6 [9, 20]. SHP2 can also form a tertiary complex with the scaffolding proteins Gab1/2 and the p85 subunit of phosphatidylinositol-3-kinase (PI3K) [27], which leads to activation of the Akt pathway. Several papers have so far reported that the PI3K/Akt pathway triggered by IL-6 plays important roles in various cells [28–32], but no reports have been published regarding the effect of IL-6 on this pathway in osteoblasts.

The purpose of this study was to clarify the effect of IL-6 on osteoblast differentiation *in vitro*, with consideration of intracellular signaling pathways in murine MC3T3-E1 osteoblastic cells and primary murine calvarial osteoblasts.

Materials and methods

Ethics statement

Prior to the study, all experimental protocols were approved by the Ethics Review Committee for Animal Experimentation of Osaka University School of Medicine.

Cell culture

MC3T3-E1 osteoblastic cells were purchased from Riken Cell Bank (Tsukuba, Japan). MC3T3-E1 cells were cultured in α -minimum essential medium (α -MEM) containing 10 % fetal bovine serum (FBS; Equitech-Bio, Kerrville, TX, USA) and 1 % penicillin and streptomycin at 37 °C in a humidified atmosphere of 5 % CO₂. All media were purchased from Life Technologies Japan (Tokyo, Japan). Murine primary osteoblasts were isolated from the calvariae of 3-day-old C57BL/6 mice (Charles River Laboratories Japan, Inc, Osaka, Japan) by sequential collagenase digestion as described previously [33].

MC3T3-E1 cells and murine calvarial osteoblasts were seeded at 1×10^5 cells per well in 12-well plates. After the cells reached confluence, the medium was replaced to induce osteoblast differentiation. The differentiation medium contained 10 % FBS, 10 mM β -glycerophosphate, and 50 μ g/ml ascorbic acid in the absence or presence of recombinant mouse (rm) IL-6 (R&D Systems, Inc., Minneapolis, MN, USA) (10, 50 ng/mL), and rm sIL-6R (R&D Systems) (100 ng/mL). The medium and reagents were renewed every 3 days.

To study signal transduction, the following inhibitors or vehicle (DMSO) (Sigma-Aldrich, St. Louis, MO, USA) were added to culture medium at several concentrations; MEK inhibitor (U0126; 1, 2.5, 5 μ M; Cell Signaling Technology, Danvers, MA, USA), STAT3 inhibitor (V Statitc; 2.5, 5 μ M; Calbiochem, La Jolla, CA, USA), PI3K inhibitor (LY294002; 1, 2.5, 5 μ M; Cell Signaling Technology), and SHP2 inhibitor (PHPS1; 5, 20, 40 μ M; Sigma-Aldrich). These inhibitors were added 1 h before treatment with IL-6/sIL-6R. All inhibitors were maintained until the end of the culture period at the indicated concentrations.

Alkaline phosphatase (ALP) staining and activity

MC3T3-E1 cells and murine calvarial osteoblasts were treated with or without IL-6/sIL-6R and signal pathway inhibitors after the cells reached confluence and were incubated for 6 days.

For ALP staining, after fixation with 10 % formalin, cells were washed twice with phosphate-buffered saline (PBS) (pH 7.4) and incubated with ALP substrate solution,

0.1 mg/ml naphthol AS-MX (Sigma-Aldrich), and 0.6 mg/ml fast violet B salt (Sigma-Aldrich) in 0.1 M Tris-HCl (pH 8.5) for 20 min.

To measure ALP activity, cells were washed twice with PBS and lysed in Mammalian Protein Extraction Reagent (Pierce, Rockford, IL, USA) according to the manufacturer's protocol. ALP activity was assayed using *p*-nitrophenylphosphate as a substrate by an Alkaline Phosphatase Test Wako (Wako Pure Chemicals Industries, Ltd., Osaka, Japan), and the protein content was measured using the Bicinchoninic Acid Protein Assay Kit (Pierce).

Proliferation assay

MC3T3-E1 cells were cultured in 96-well plates at a concentration of 2.0×10^4 cells/cm² in α -MEM containing 10 % FBS. Cells were incubated for 1 day, after which the medium was treated with IL-6/sIL-6R for 3 days. Cell proliferation was assessed using the Premix WST-1 Cell Proliferation Assay System (Takara Bio, Inc., Otsu, Japan) according to the manufacturer's instructions. We performed this assay every 24 h.

Alizarin red staining

After fixation with 10 % formalin, MC3T3-E1 cells and murine calvarial osteoblasts were washed with distilled water, and stained with alizarin red S solution (Sigma-Aldrich) (pH 6.0) for 10 min, followed by incubation in 100 mM cetylpyridinium chloride for 1 h at room temperature to dissolve and release calcium-bound alizarin red. The absorbance of the released alizarin red was then measured at 570 nm [34]. To measure the value of absorbance for alizarin red, the absorbance data were normalized by total DNA content. Total DNA was extracted using a DNeasy Blood & Tissue Kit (Qiagen, Düsseldorf, Germany).

Knockdown of MEK1, MEK2, Akt1 and Akt2 using RNA interference

MC3T3-E1 cells were transfected with small interfering RNAs (siRNA) using Lipofectamine RNAiMAX (Life Technologies Japan) according to the reverse transfection method in the manufacturer's protocol.

The siRNAs for MEK2, Akt1 and Akt2 and that for MEK1 were purchased from Cell Signaling Technology and Qiagen, respectively, with negative controls for each molecule. MC3T3-E1 cells transfected with siRNA were seeded in 24-well plates at a concentration of 1.0×10^4 cells/cm² for 48 h. The medium was then replaced with differentiation medium with vehicle or with 20 ng/ml IL-6 and 100 ng/ml sIL-6R and the cells were incubated for 3 days prior to use for further experiments.

Western blotting

Cells cultured in 6-well plates for 2 days were washed twice with PBS and then homogenized with 100 μ l of Kaplan buffer (150 mM NaCl, 50 mM Tris-HCl pH 7.4, 1 % NP40, 10 % glycerol, and 1 tablet per 50 ml buffer of protease inhibitor cocktail and phosphatase inhibitor cocktail). The lysates were centrifuged at 13,000 rpm for 20 min at 4 °C, and the supernatants were used for electrophoresis after a protein assay using bovine serum albumin as standard. Western blotting was performed by use of the following antibodies purchased from Cell Signaling Technology, except for phosphate anti-Akt2 antibody from Enogene Biotech (New York, NY, USA): phosphate anti-STAT3 (Tyr705) (1:2000) and anti-STAT3 (1:1000); phosphate anti-Akt (Ser473) (1:2000), phosphate anti-Akt2 (Ser474) (1:1000), anti-Akt1, anti-Akt2, and anti-Akt (1:1000); phosphate anti-ERK (Thr202/Tyr204) (1:2000), anti-MEK1, anti-MEK2 and anti-ERK (1:1000); and phosphate anti-SHP2 (Tyr542) (1:1000). To control for protein loading, blots were additionally stained with anti- β actin antibody (1:1000).

Reverse transcription polymerase chain reaction (RT-PCR)

Total RNA was extracted from cells with an RNeasy Mini Kit (Qiagen), and first-strand cDNA was synthesized using SuperScript II RNase H-reverse transcriptase (Life Technologies Japan). Then PCR was performed using Ex Taq (Takara Bio) and the following primers:

Osteocalcin (forward primer 5'-CTCACTCTGCTGGCC CTG-3'; reverse primer 5'-CCGTAGATGCGTTTGTAGGC-3');

Osterix (forward primer 5'-AGGCACAAAGAAGCCATAC-3'; reverse primer 5'-AATGAGTGAGGGAAGGG T-3');

Runx2 (forward primer 5'-GCTTGATGACTCTAAACC TA-3'; reverse primer 5'-AAAAAGGGCCAGTTCTGAA-3');

GAPDH (forward primer 5'-TGAACGGGAAGCTCAC TGG-3'; reverse primer 5'-TCCACCACCCTGTTGCTG TA-3').

Quantitative real-time PCR analysis

We obtained cDNA by reverse transcription as mentioned above, and proceeded with real-time PCR using a Light Cycler system (Roche Applied Science, Basel, Switzerland). The SYBR Green assay using a Quantitect SYBR Green PCR Kit (Qiagen), in which each cDNA sample was evaluated in triplicate 20- μ l reactions, was used for all

target transcripts. Expression values were normalized to GAPDH.

Statistical analysis

The results are expressed as the mean \pm standard error (SE). Between-group differences were assessed using the ANOVA test. A probability value of <0.05 was considered to indicate statistical significance.

Results

IL-6/sIL-6R does not affect proliferation, but significantly reduces ALP activity and expression of osteoblastic genes in MC3T3-E1 cells

We first measured the proliferation of MC3T3-E1 cells with IL-6. Cell proliferation did not show significant difference in any culture condition (Fig. 1a).

To investigate the influence of IL-6 treatment on osteoblast differentiation, we examined ALP activity in MC3T3-E1 cells. As shown in Fig. 1b and c, IL-6/sIL-6R significantly reduced ALP activity in a dose-dependent manner. The single addition of sIL-6R did not show a significant difference as compared to the negative control with vehicle. As shown in Fig. 1d and e, gene expression of Runx2, osterix and osteocalcin was significantly down-regulated by IL-6/sIL-6R in a dose-dependent manner. Again, the single addition of sIL-6R did not show significant difference as compared to the negative control with vehicle.

IL-6/sIL-6R significantly inhibits mineralization of extracellular matrix (ECM) in MC3T3-E1 cells

As shown in Fig. 2a, IL-6/sIL-6R significantly inhibited the mineralized area in a dose-dependent manner. The single addition of sIL-6R did not show a significant difference as compared to the negative control with vehicle (Fig. 2a). Quantitative analysis of mineralization by measuring the absorbance of alizarin red revealed a significant decrease by IL-6/sIL-6R in a dose-dependent manner (Fig. 2b).

IL-6/sIL-6R activates ERK, STAT3 and Akt2 signal transduction pathways in MC3T3-E1 cells

When MC3T3-E1 cells were incubated in the presence of IL-6/sIL-6R, phosphorylation of ERK, STAT3 and Akt was clearly observed at 15 min, and their activation became weaker at 30 min. When only sIL-6R was added, there was no apparent activation of ERK, STAT3, or Akt as

compared to the negative control (Fig. 3a). As for Akt, the phosphorylation by IL-6/sIL-6R was recognized more strikingly as early as 5 min in a dose-dependent manner, both for whole and for Akt2 only, one of its three isoforms (Fig. 3b).

IL-6-induced activation of ERK is enhanced by blocking the STAT3 signaling pathway, and IL-6-induced ERK and Akt signaling pathways negatively regulate each other reciprocally

The SHP2 inhibitor PHPS1 [35] inhibited IL-6-induced phosphorylation of ERK and Akt to the constitutive level, but did not inhibit STAT3 (Fig. 4a and Supplementary Fig. S1a), suggesting that the downstream pathways of SHP2 are ERK and Akt, not STAT3. The STAT3 inhibitor V Static inhibited the phosphorylation of STAT3 but enhanced ERK significantly (Fig. 4a and Supplementary Fig. S1a), suggesting that STAT3 could negatively regulate ERK, which is consistent with previous reports [36]. The MEK/ERK inhibitor U0126 completely inhibited both constitutive and IL-6-induced phosphorylation of ERK but enhanced those of Akt. Moreover, the PI3K/Akt inhibitor LY294002 completely inhibited both constitutive and IL-6-induced phosphorylation of Akt but enhanced those of ERK (Fig. 4b and Supplementary Fig. S1b). From these findings, we concluded that IL-6-induced ERK and Akt signaling pathways, both of which are downstream of SHP2, can negatively regulate each other reciprocally.

The negative effects of IL-6 on osteoblast differentiation are restored by inhibition of MEK, PI3K and SHP2, while they are enhanced by inhibition of STAT3

To identify the intracellular signaling pathways associated with the downregulation of osteoblast differentiation, the effects of various signal transduction inhibitors, consisting of a MEK inhibitor (U0126), PI3K inhibitor (LY294002), SHP2 inhibitor (PHPS1), and STAT3 inhibitor (V Static), were assessed for ALP activity, the expression of osteoblastic genes (Runx2, osterix and osteocalcin), and the mineralization of ECM.

The negative effect of IL-6/sIL-6R on ALP activity was restored by treatment with either U0126, LY294002, or PHPS1 in a dose-dependent manner. On the other hand, the negative effect of IL-6/sIL-6R on ALP activity was enhanced by treatment with V Static (Fig. 5a). These results indicate that the SHP2-associated signal transduction molecules MEK/ERK and PI3K/Akt have a negative effect on osteoblast differentiation, whereas the JAK-associated molecule STAT3 has a positive effect.

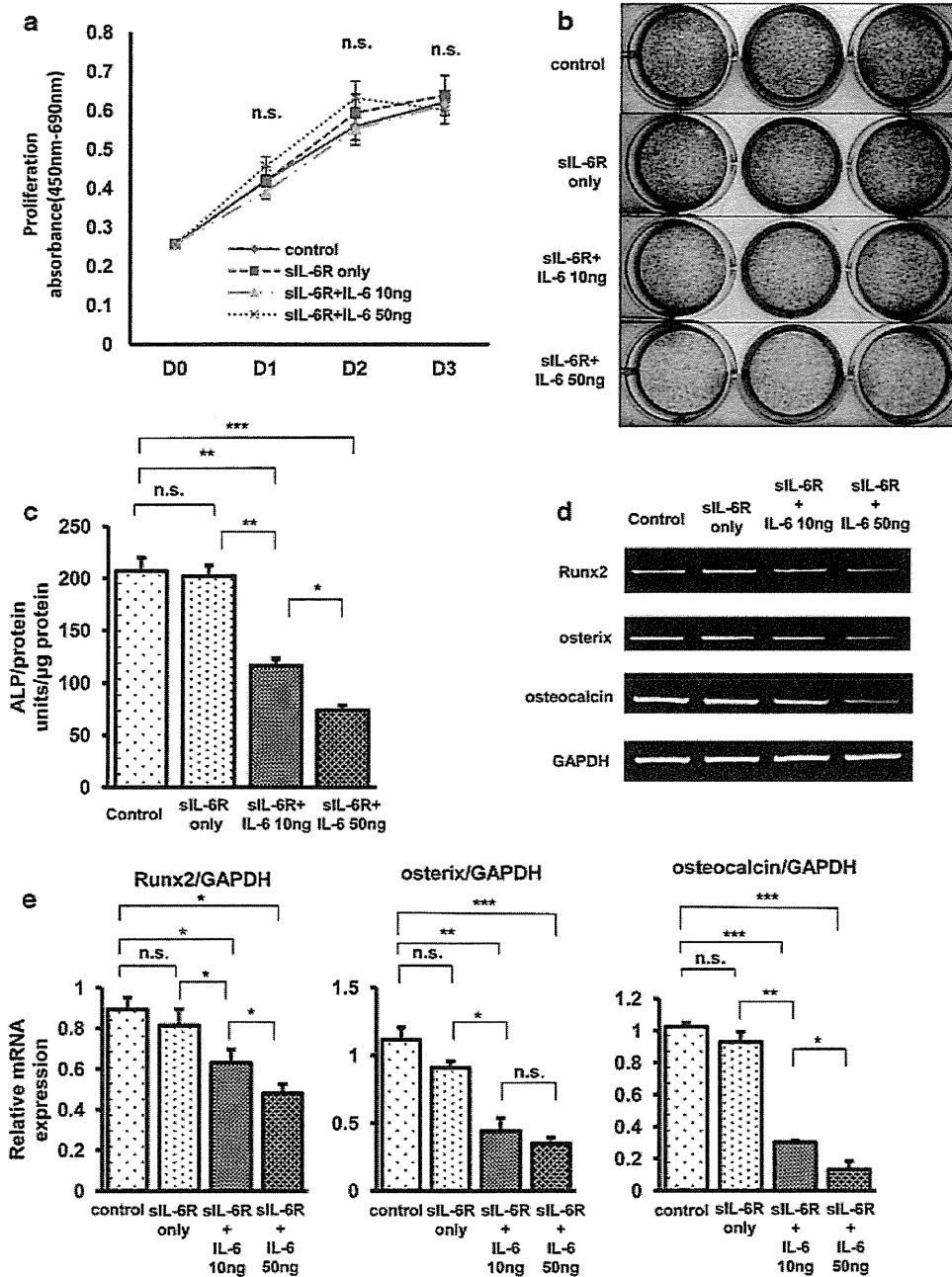


Fig. 1 IL-6/siL-6R significantly reduced ALP activity and expression of osteoblastic genes in MC3T3E1 cells, but did not affect proliferation. **a** Proliferation of MC3T3E1 cells with IL-6/siL-6R was examined. Cells were pre-incubated for 1 day and then the medium was treated with or without IL-6/siL-6R for 3 days. Cell proliferation assay was performed daily throughout the 4 days of incubation. Cell proliferation did not show significant differences in any culture condition. **b** ALP staining was performed in MC3T3E1 cells treated with or without IL-6/siL-6R for 6 days. Apparently significant reduction of ALP staining was recognized in cells treated with either 10 or 50 ng/ml IL-6. **c** ALP activity of the lysates of MC3T3E1 cells treated with or without IL-6/siL-6R for 6 days was measured using p-nitrophenylphosphate as a substrate. IL-6/siL-6R significantly reduced ALP activity in a dose-dependent manner.

d Total RNA was extracted from MC3T3E1 cells treated with or without IL-6/siL-6R for 6 days and subjected to RT-PCR for osteoblastic genes Runx2, osterix, and osteocalcin. Apparently significant reduction of osteoblastic gene expression was recognized in cells treated with either 10 or 50 ng/ml IL-6. **e** Real-time PCR for Runx2, osterix, and osteocalcin was performed for quantitative analysis. Data were normalized to GAPDH expression and are shown as the ratio of expression compared to control cells treated with vehicle. The expression of osteoblastic genes was significantly downregulated by IL-6/siL-6R in a dose-dependent manner. Representative data from at least 3 independent experiments are shown. Data are shown as mean \pm SE. *n.s.* not significant; **P* < 0.05; ***P* < 0.001; ****P* < 0.001

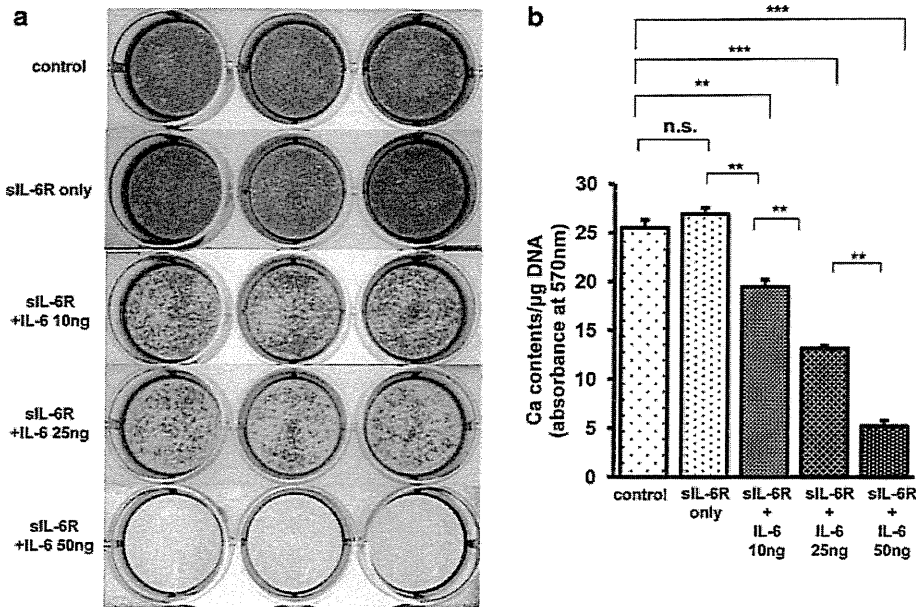


Fig. 2 IL-6/sIL-6R significantly inhibited the mineralization of ECM in MC3T3E1 cells. MC3T3-E1 cells were treated with or without IL-6/sIL-6R and were incubated for 21 days. **a** After fixation, the cells were stained with alizarin red solution. Apparently significant reduction of alizarin red staining was recognized in the cells treated with either 10, 25, or 50 ng/ml IL-6. **b** Matrix

mineralization was quantified by the measurement of absorbance of alizarin red and normalized by total DNA content. Matrix mineralization was significantly reduced by IL-6/sIL-6R in a dose-dependent manner. Representative data from at least 3 independent experiments are shown. Data are shown as mean \pm SE. *n.s.* not significant; **P* < 0.05; ***P* < 0.001; ****P* < 0.001

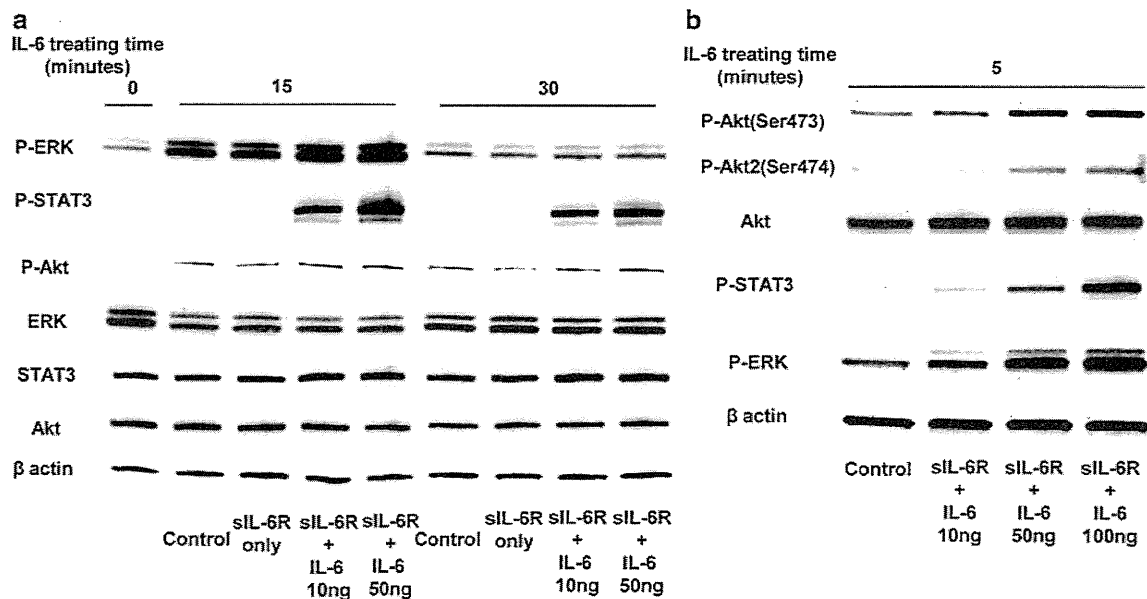


Fig. 3 IL-6/sIL-6R-activated ERK, STAT3, and Akt2 signal transduction pathways in MC3T3-E1 cells. **a** MC3T3-E1 cells were treated with vehicle or with 10 or 50 ng/ml IL-6 and 100 ng/ml sIL-6R in a time-course experiment (0, 15, and 30 min). Western blot analysis was performed using cell lysates for the detection of ERK, STAT3, and Akt, either phosphorylated or not. IL-6/sIL-6R significantly induced the phosphorylation of ERK, STAT3, and Akt in a dose-dependent manner. **b** MC3T3-E1 cells were incubated with increasing

concentrations of IL-6 and 100 ng/ml sIL-6R for 5 min. Western blotting was performed using cell lysates for the detection of ERK, STAT3, as well as Akt, either non-phosphorylated, phosphorylated, or the phosphorylated isoform Akt2. The phosphorylation of both whole Akt and Akt2 by IL-6/sIL-6R was recognized more strikingly in a dose-dependent manner. Representative data from at least three independent experiments are shown

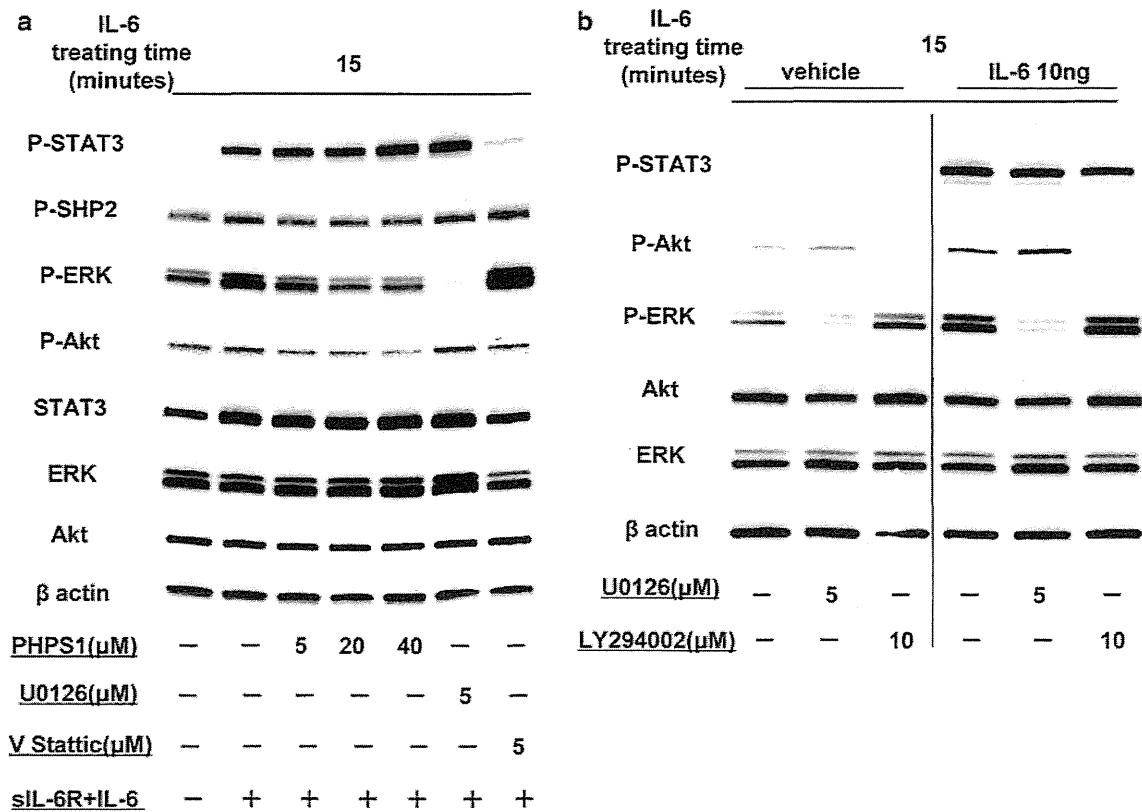


Fig. 4 IL-6-induced activation of ERK was enhanced by blocking the STAT3 signaling pathway, and IL-6-induced ERK and Akt signaling pathways negatively regulated each other reciprocally. **a** MC3T3-E1 cells were stimulated with 10 ng/ml IL-6 and 100 ng/ml sIL-6R (15 min) after pretreatment either with PHPS1 (5, 20, 40 μM; 1 h), with U0126 (5 μM; 1 h), or with V Stattic (5 μM; 1 h), and the cell lysates were subjected to Western blotting. PHPS1 inhibited IL-6-induced phosphorylation of ERK and Akt to the constitutive level, but

not of STAT3. IL-6-induced activation of ERK was enhanced by V Stattic. **b** MC3T3-E1 cells were treated with vehicle or with 10 ng/ml IL-6 and 100 ng/ml sIL-6R (15 min) after pretreatment either with U0126 (5 μM; 1 h) or with LY294002 (10 μM; 1 h), and the cell lysates were subjected to Western blotting. Both constitutive and IL-6-induced phosphorylation of Akt and ERK were enhanced by treatment with U0126 and LY294002, respectively. Representative data from at least three independent experiments are shown

The negative effect of IL-6/sIL-6R on the expression of osteoblastic genes (Runx2, osterix and osteocalcin) was also restored by treatment with either U0126, LY294002, or PHPS1 in a dose-dependent manner, while it was enhanced by treatment with V Stattic (Fig. 5b). Moreover, a high dose of PHPS1, 20 μM, caused significantly upregulated expression of osteocalcin.

For mineralization of ECM, the negative effect of IL-6/sIL-6R was restored by treatment with either U0126, LY294002, or PHPS1. As with ALP activity and osteoblastic gene expression, the negative effect of IL-6/sIL-6R on mineralization was enhanced by treatment with V Stattic (Fig. 6a, b). ALP activity, osteoblastic gene expression, and mineralization of ECM in cells treated only with each inhibitor demonstrated the same behavior (Figs. 5, 6).

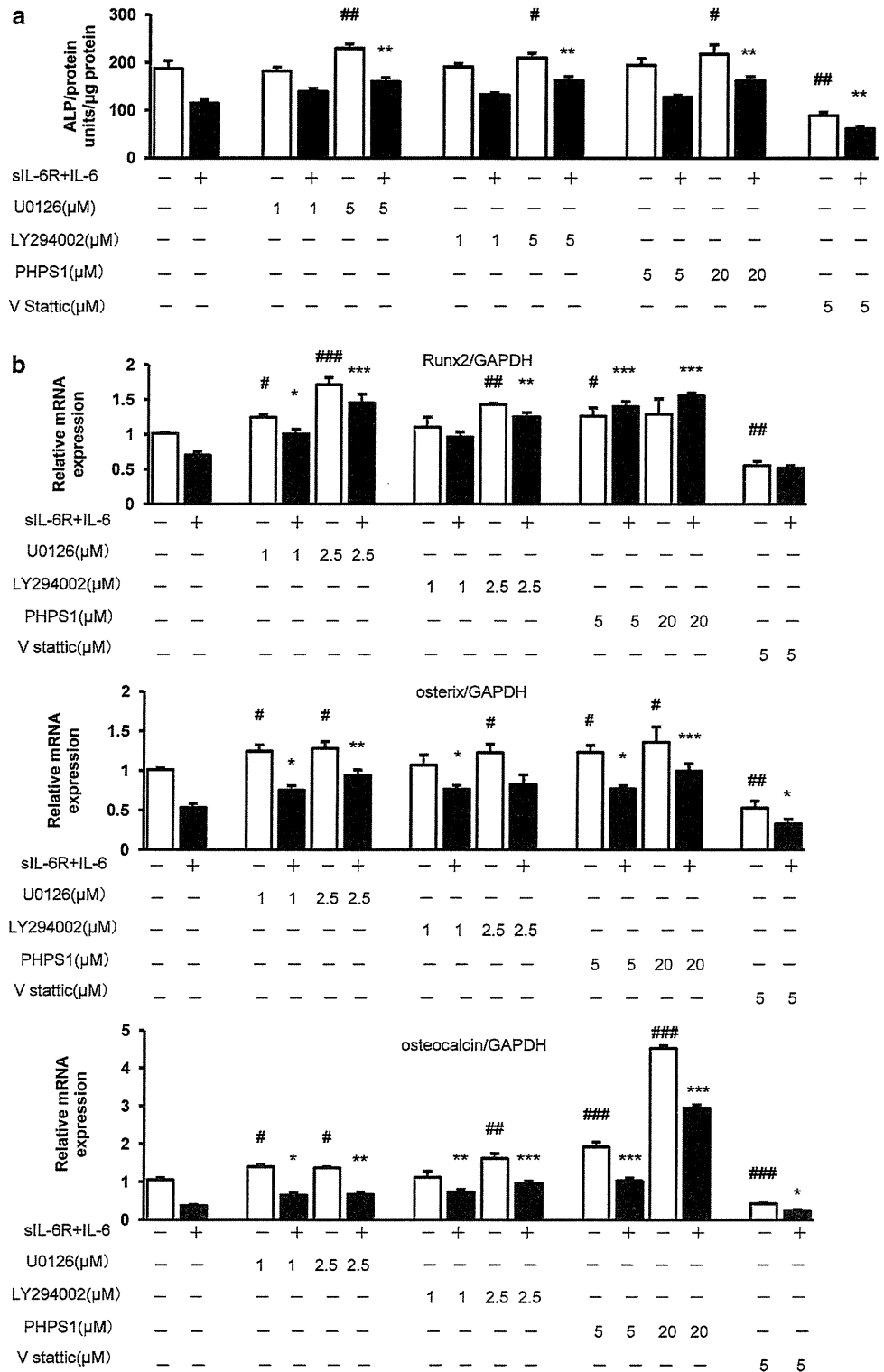
Furthermore, the negative effects of ALP activity, osteoblastic gene expression and mineralization of ECM by stimulation with IL-6/sIL-6R were compared for levels in the presence and in the absence of each inhibitor. The

negative effects on osteoblast differentiation by IL-6/sIL-6R showed a tendency to decrease in the presence of each inhibitor, as compared to the absence of inhibitors (Figs. 5, 6). The negative effects were decreased by 15–44, 20–61, 7–140, and 21–80 % in the presence of U0126, LY294002, PHPS1 and V Stattic, respectively, as compared to the absence of inhibitors. These results indicate that the effects of IL-6/sIL-6R on osteoblast differentiation might be mediated either by MEK/ERK, PI3K/Akt, or JAK/STAT3 pathways.

Knockdown of MEK2 and Akt2 via siRNA transfection restores ALP activity and Runx2 gene expression

To further confirm the effects of MEK and Akt inhibition on osteoblast differentiation in MC3T3-E1 cells, we studied cell differentiation after knockdown of MEK and Akt. For each protein, RNAs of two isoforms were separately blocked: MEK1 and MEK2 for MEK, and Akt1 and Akt2 for Akt.

Fig. 5 The negative effects of IL-6 on ALP activity and the expression of osteoblastic genes were restored by inhibition of MEK, PI3K, and SHP2, while they were enhanced by inhibition of STAT3. MC3T3-E1 cells were pretreated either with U0126 (1, 2.5, 5 μ M; 1 h), LY294002 (1, 2.5, 5 μ M; 1 h), PHPS1 (5, 20 μ M; 1 h), or V Static (5 μ M; 1 h), then stimulated either with 10 ng/ml IL-6 and 100 ng/ml sIL-6R or with vehicle and incubated for 6 days. **(a)** ALP activity of the cell lysates was measured using p-nitrophenylphosphate as a substrate. The negative effect of IL-6 on ALP activity was restored by treatment with either U0126, LY294002, or PHPS1 in a dose-dependent manner, while it was enhanced by treatment with V Static. **(b)** Total RNA was extracted and real-time PCR for Runx2, osterix, and osteocalcin was performed. Data were normalized to GAPDH expression and are shown as the ratio of gene expression compared to control cells treated with vehicle. The negative effect of IL-6 on expression of osteoblastic genes was restored by treatment either with U0126, LY294002, or PHPS1 in a dose-dependent manner, while it was enhanced by treatment with V Static. Representative data from at least three independent experiments are shown. Data are shown as mean \pm SE. *n.s.* not significant; $^{\#}P < 0.05$; $^{\#\#}P < 0.001$; $^{\#\#\#}P < 0.001$, compared to the group treated with vehicle. $^*P < 0.05$; $^{**}P < 0.001$; $^{***}P < 0.001$, compared to group treated with IL-6/sIL-6R



The protein expression level of each molecule was found to be diminished selectively at 48 h after transfection of the respective siRNAs (Fig. 7a). The ALP activity in MC3T3-E1 cells treated with IL-6/sIL-6R was restored by knockdown of MEK2 and Akt2 as compared to that in cells transfected with negative control siRNA.

On the other hand, knockdown of MEK1 and Akt1 enhanced the negative effects of IL-6/sIL-6R on ALP activity (Fig. 7b) (ALP activity after transfection with each siRNA without IL-6/sIL-6R demonstrated the same behavior; Fig. 7b) Quantitative real-time PCR analysis revealed that the gene expressions of Runx2, osterix, and

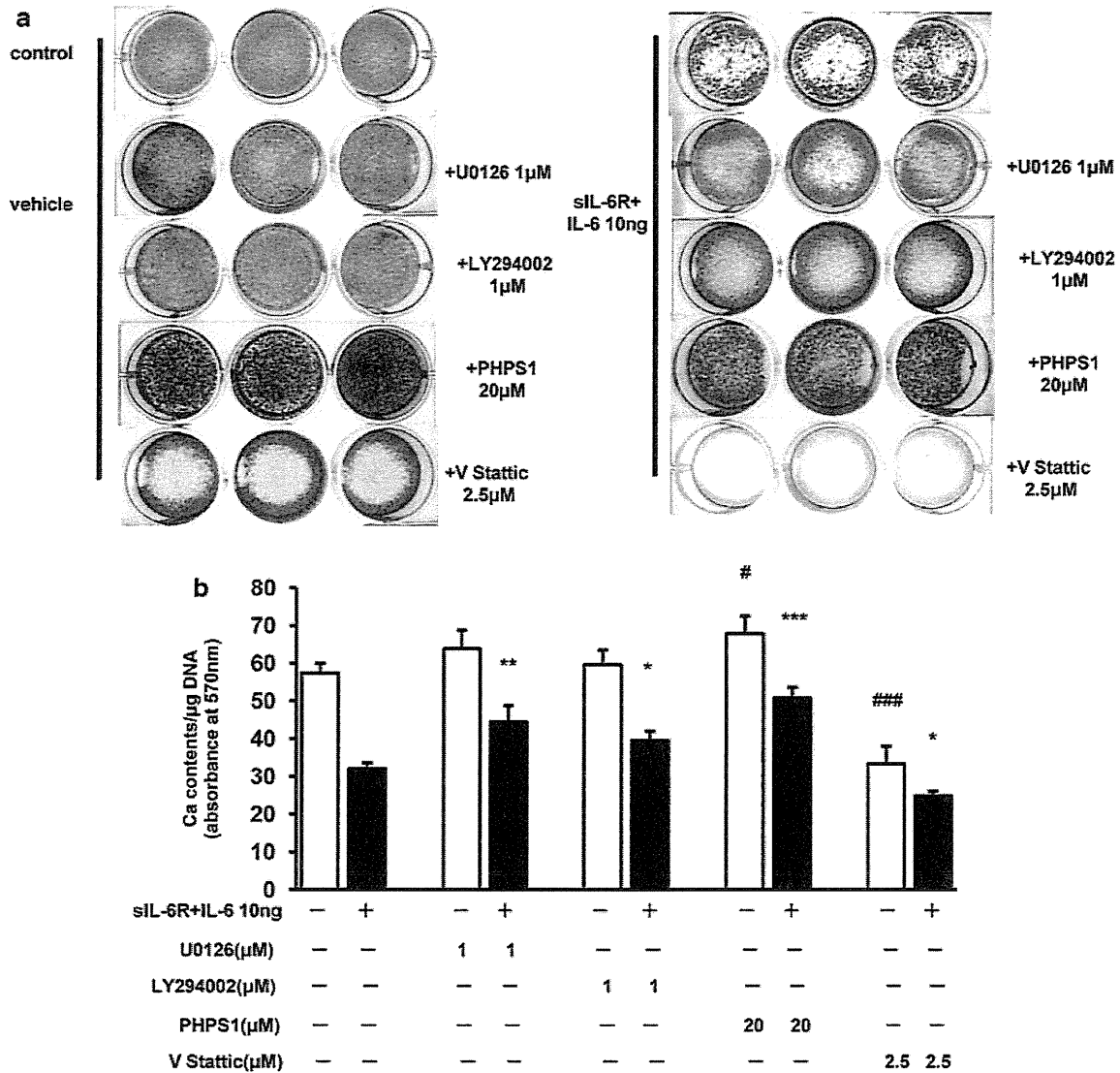


Fig. 6 The negative effect of IL-6 on mineralization of ECM was restored by inhibition of MEK, PI3K, and SHP2, while it was enhanced by inhibition of STAT3. MC3T3-E1 cell were pretreated either with U0126 (1 μM; 1 h), LY294002 (1 μM; 1 h), PHPS1 (20 μM; 1 h), or V Stattic (2.5 μM; 1 h), then stimulated with either 10 ng/ml IL-6 and 100 ng/ml sIL-6R or with vehicle and incubated for 21 days. **a** After fixation, the cells were stained with alizarin red solution. The reduction of alizarin red staining by IL-6/sIL-6R was restored in cells treated with either U0126, LY294002, or PHPS1, while it was enhanced in those treated with V Stattic. **b** Quantification

of matrix mineralization was by measurement of absorbance for alizarin red normalized by total DNA content. The reduction of matrix mineralization by IL-6/sIL-6R was restored in cells treated with either U0126, LY294002, or PHPS1, while it was enhanced in those treated with V Stattic. Representative data from at least three independent experiments are shown. Data are shown as mean ± SE. *n.s.* not significant; #*P* < 0.05; ###*P* < 0.001; ####*P* < 0.001, compared to the group treated with vehicle. **P* < 0.05; ***P* < 0.001; ****P* < 0.001, compared to group treated with IL-6/sIL-6R

osteocalcin were restored by knockdown of MEK2. On the other hand, knockdown of Akt2 also restored Runx2, but decreased osteocalcin expression (Fig. 7c), while knockdown of Akt2 without IL-6/sIL-6R caused no significant difference in Runx2 expression (Fig. 7b). As was recognized for ALP activity, knockdown of MEK1 and Akt1 enhanced the downregulation of osteocalcin expression (Fig. 7b, c). Also, the negative effects of IL-6/

sIL-6R on osteoblast differentiation showed some tendency to decrease with each knockdown compared to those without knockdown. The negative effects were decreased by 2–24, 4–27, 7–43, and 21–26 % with knockdown of MEK1, MEK2, Akt1, and Akt2, respectively, as compared to those without knockdown. These results indicate that IL-6 may suppress osteoblast differentiation through MEK2 and Akt2.

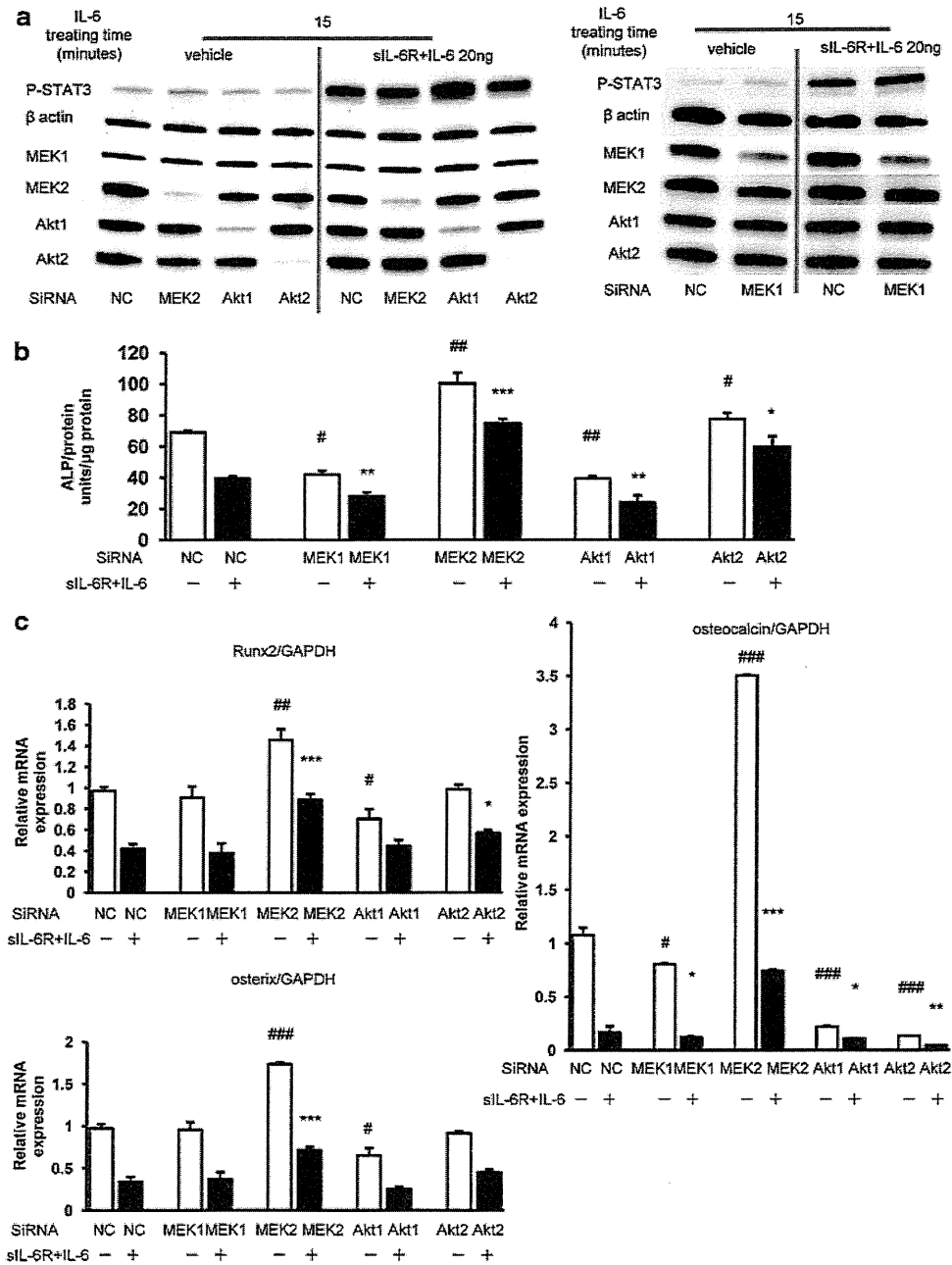


Fig. 7 Knockdown of MEK2 and Akt2 in cells transfected with siRNA restored ALP activity and Runx2 gene expression. **a** MC3T3-E1 cells transfected with respective siRNAs were cultured for 48 h. Western blotting was performed using cell lysates stimulated with vehicle or with 20 ng/ml IL-6 and 100 ng/ml sIL-6R (15 min). Expression levels of each protein, MEK1, MEK2, Akt1, and Akt2, were selectively diminished at 48 h after transfection with respective siRNAs. **b** MC3T3-E1 cells transfected with respective siRNAs were incubated for 48 h after which the medium was changed to differentiation medium with vehicle or with 20 ng/ml IL-6 and 100 ng/ml sIL-6R. The cells were then incubated for 3 days to evaluate osteoblast differentiation. ALP activity in MC3T3-E1 cells treated with IL-6/sIL-6R was restored by knockdown of MEK2 and

Akt2 as compared to that in cells transfected with negative control siRNA. **c** Expression of osteoblastic genes in MC3T3-E1 cells transfected with respective siRNAs was assessed by real-time PCR. The expression of each gene was normalized against GAPDH expression. The gene expressions of Runx2, osterix, and osteocalcin were restored by knockdown of MEK2. Knockdown of Akt2 also restored Runx2, but decreased osteocalcin. Representative data from at least three independent experiments are shown. Data are shown as mean ± SE. *n.s.* not significant; #*P* < 0.05; ##*P* < 0.001; ###*P* < 0.001, compared to negative control group treated with vehicle. **P* < 0.05; ***P* < 0.001; ****P* < 0.001, compared to negative control group treated with IL-6/sIL-6R

IL-6/sIL-6R inhibits the differentiation of primary murine calvarial osteoblasts by activating phosphorylation of ERK, Akt2, and STAT3

Experiments were repeated with murine calvarial osteoblasts isolated from the calvariae of 3-day-old C57BL/6 mice. As was recognized in MC3T3-E1 cells, IL-6 inhibited ALP activity (Fig. 8a), the expression of osteoblastic genes (Fig. 8b), and mineralization (Fig. 8c, d) in a dose-dependent manner. Furthermore, IL-6 induced phosphorylation of ERK, Akt2, and STAT3 (Fig. 8e), which was exactly the same as with MC3T3-E1 cells.

Discussion

We examined the effects of IL-6 and its soluble receptor on the proliferation and differentiation of murine MC3T3-E1 osteoblastic cells and primary murine calvarial osteoblasts. Our results showed that they significantly reduced ALP activity, bone mineralization, and expression of the osteoblastic genes Runx2, Osterix, and osteocalcin, in a dose-dependent manner. From these experiments, we clearly demonstrated that IL-6 inhibited osteoblast differentiation of MC3T3-E1 cells and primary murine calvarial osteoblasts.

It has been demonstrated that the JAK/STAT3 signaling pathway has important roles both, *in vivo* and *in vitro*, in the differentiation of osteoblasts [37, 38]. Our results are consistent with previous reports and imply that the activation of STAT3 induced by IL-6 may induce osteoblast differentiation.

IL-6 activates another major intracellular signaling pathway, SHP2/ERK, and can also lead to the activation of an additional signaling cascade involving SHP2/PI3K/Akt. IL-6-induced activation of PI3K and downstream protein kinase Akt/PKB has been reported to play important roles in the proliferation of prostate cancer cells [30, 31], hepatoma cells [32], and multiple myeloma cells [29]. They were also reported to associate with neuroendocrine differentiation of prostate cancer cells induced by IL-6 [32]. In this study, we focused on the PI3K/Akt pathway triggered by IL-6, because no reports have demonstrated the role of IL-6 in the activation of PI3K/Akt signaling pathway in osteoblasts. We have demonstrated for the first time that IL-6-induced activation of Akt2, one of the downstream pathways of SHP2, may be a key player in the negative regulation of osteoblast differentiation induced by IL-6. Among the three isoforms of Akt, Akt1 and Akt2 are highly expressed in osteoblasts [39]. Mice lacking Akt1, the major isoform in bone tissue, exhibit osteopenia [40, 41], and the impact of Akt1 deficiency in osteoblast differentiation and bone development have also been

published [39, 42–44], all of which are consistent with our results showing that knockdown of Akt1 signaling by siRNA inhibited osteoblast differentiation. In contrast, Mukherjee et al. [44] reported enhanced osteogenic differentiation in the absence of Akt1 in cell lines. Moreover, they reported that Akt2 was required for BMP2-initiated osteoblast differentiation of cultured murine mesenchymal stem cells, but that Akt1 was dispensable in this assay [45], which is inconsistent with our results showing that knockdown of Akt2 signaling by siRNA promoted osteoblast differentiation. These discrepancies might be due to the difference between cell types, i.e. intramembranous (calvariae) cells and endochondral (long bones) cells.

In this study, gene expression of osteocalcin, a late osteoblastic differentiation marker, was upregulated by treatment with a PI3K/Akt inhibitor, but was downregulated by knockdown of both Akt1 and Akt2. Moreover, a complete blockade with a high dose (more than 10 μ M) of the PI3K/Akt inhibitor conversely downregulated the expression of osteocalcin (data not shown). This discrepancy may be due to the difference between the temporary or partial blockade by the inhibitor and constitutive knockdown by siRNA. Since bone formation has been reported to increase without impairment of mineralization and resorption even in osteocalcin-deficient mice [46], the expression of osteocalcin may not directly affect bone formation.

We have previously reported that osteoblast differentiation was significantly promoted by MEK inhibitor in BMP-2-treated C2C12 cells and MC3T3-E1 cells [47]. Our findings in the present study are consistent with our previous report and others [47–49] at the point that IL-6-induced activation of ERK significantly downregulated osteoblast differentiation. In addition, our results suggest that there might be different roles in osteoblast differentiation between MEK1 and MEK2. Constitutively active expression of MEK1 has been reported to accelerate bone development both *in vitro* [50] and *in vivo* [51], which is consistent with the results showing that knockdown of MEK1 inhibited osteoblast differentiation in the present study. As for MEK2, there are no reports concerning its roles in osteoblast differentiation, and we are the first to demonstrate that MEK2 may also be a key player in the negative regulation of osteoblast differentiation induced by IL-6. The effects of an MEK inhibitor that inhibits both MEK1 and MEK2 on bone formation are still controversial [52]. These controversies might be due to different roles played between MEK1 and MEK2 in osteoblast differentiation, and the effects of MEK inhibitors could depend on which pathway is predominantly inhibited in each study.

With respect to intracellular signaling pathways, our results showed that IL-6 triggers three signaling pathways, one of which has a conflicting function with the others.

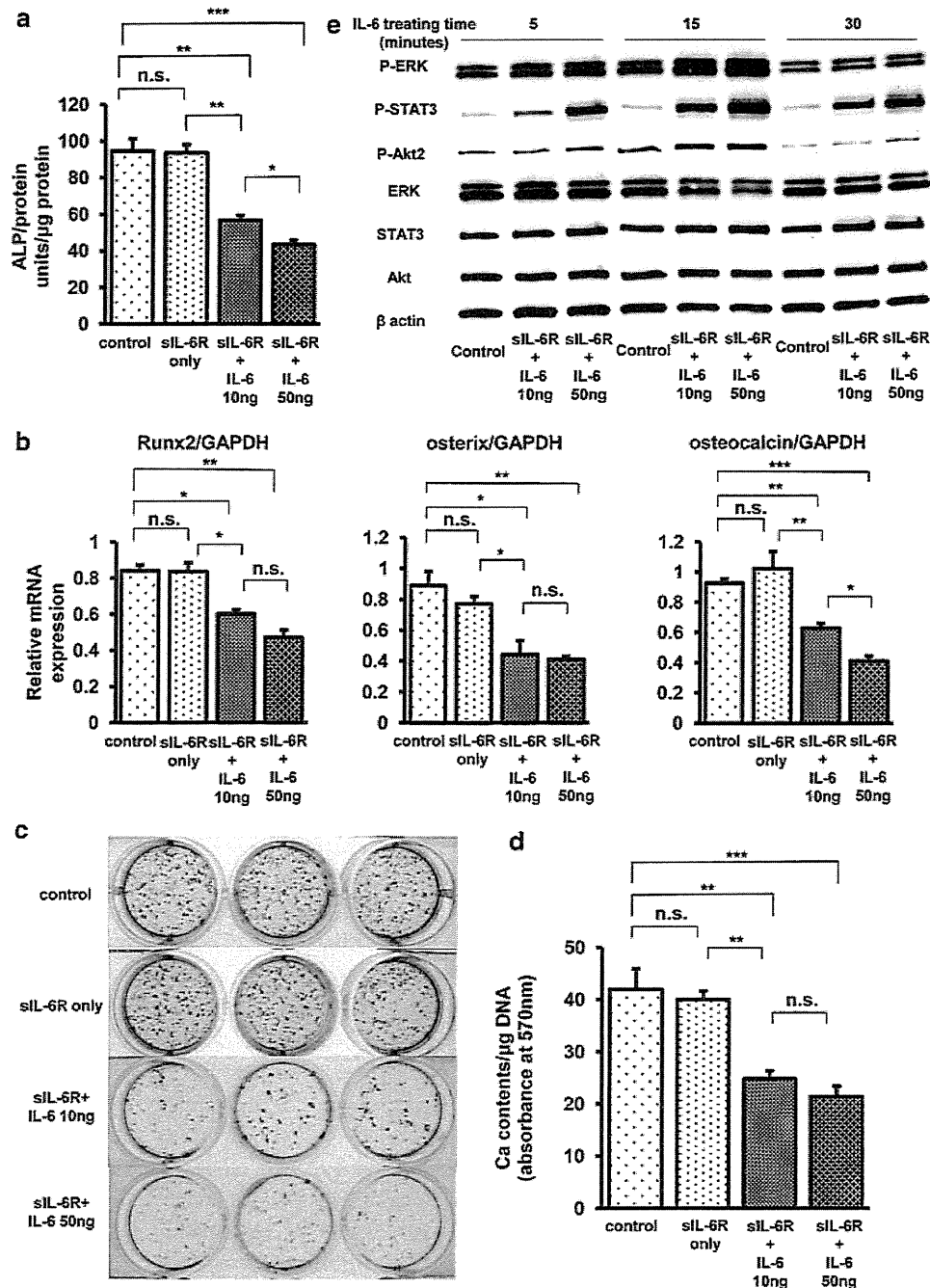
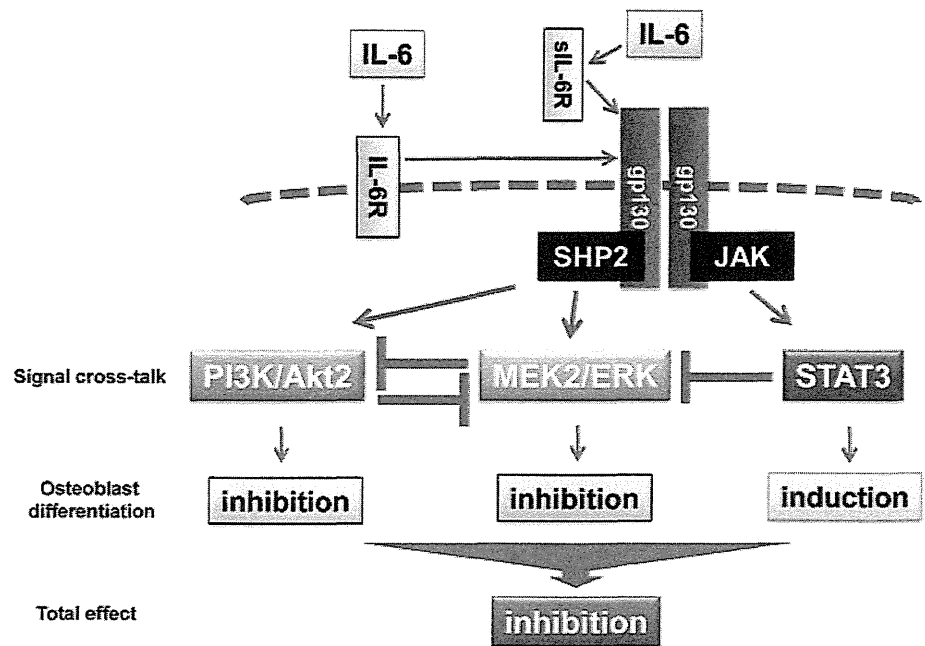


Fig. 8 IL-6/siL-6R inhibited the differentiation of primary murine calvarial osteoblasts with the activated phosphorylation of ERK, Akt2, and STAT3. **a** ALP activity of lysates of murine calvarial osteoblasts treated with or without IL-6/siL-6R for 6 days was measured using p-nitrophenylphosphate as a substrate. IL-6/siL-6R significantly reduced ALP activity in a dose-dependent manner. **b** Total RNA was extracted from murine calvarial osteoblasts treated with or without IL-6/siL-6R for 6 days, and real-time PCR for Runx2, osterix, and osteocalcin was performed. Data were normalized to GAPDH expression and are shown as the ratio of gene expression as compared to control cells treated with vehicle. The expression of osteoblastic genes was significantly downregulated by IL-6/siL-6R in a dose-dependent manner. **c** Murine calvarial osteoblasts were treated with or without IL-6/siL-6R and were cultured for 21 days. After

fixation, the cells were stained with alizarin red solution. Apparently significant reduction of alizarin red staining was recognized in cells treated with either 10 or 50 ng/ml IL-6. **d** Matrix mineralization was quantified by measurement of absorbance for alizarin red normalized by total DNA content. IL-6/siL-6R significantly inhibited mineralization of ECM in a dose-dependent manner. **e** Primary murine calvarial osteoblasts were treated with vehicle or 10 or 50 ng/ml IL-6 and 100 ng/ml siL-6R in a time-course experiment (5, 15, and 30 min). Western blotting was performed using cell lysates. IL-6 significantly induced the phosphorylation of ERK, Akt2, and STAT3 in a dose-dependent manner. Representative data from at least three independent experiments are shown. Data are shown as mean \pm SE. n.s. not significant; * P < 0.05; ** P < 0.001; *** P < 0.001

Fig. 9 Schematic presentation of signaling pathways involved in osteoblast differentiation induced by IL-6. IL-6-induced novel SHP2/MEK2/ERK and SHP2/PI3K/Akt2 signal crosstalk in osteoblastic cells; ERK and Akt signaling pathways, both of which are downstream of SHP2, negatively regulate each other reciprocally. On the other hand, the STAT3 signaling pathway negatively regulates the ERK signaling pathway. MEK2/ERK and PI3K/Akt2 have negative effects on osteoblast differentiation, whereas STAT3 has a positive effect. Overall, IL-6 inhibits osteoblast differentiation through MEK2 and Akt2 signaling pathways



SHP2/ERK and SHP2/Akt2 negatively affects osteoblast differentiation, whereas JAK/STAT3 positively affects it (Fig. 9). In other cells, it is often that simultaneous activation of the SHP2/ERK and JAK/STAT3 cascades generate opposing, or at least different signals. In osteoclasts, for example, SHP2/ERK activation inhibits osteoclastogenesis [53], whereas STAT3 is a pro-osteoclastic molecule after phosphorylation on serine727 [54]. In myeloid leukemic M1 cells, STAT3 induces differentiation in vitro [55], whereas the SHP2/ERK pathway promotes their proliferation [56]. These examples suggest that the integration of opposing activities transduced by more than one pathway could provide a biologically balanced state in the end, leaving availability to respond to another physiological situation. Indeed, Hirano and colleagues [57] have proposed a “signaling orchestration” model in a single cell, where the balance or interplay of simultaneously generated contradictory signals eventually determines the biological outcome. Thus, the inconsistent results regarding the effects of IL-6 on osteoblast differentiation in previous reports could be explained by which intracellular signaling pathway was predominantly activated in each study. The balance of three signaling pathways could be influenced by such conditions as the variety of cultured cells, the stage of cell differentiation, and the employed culture conditions.

To the best of our knowledge, this is the first report of signal crosstalk in which IL-6-induced ERK and Akt signaling pathways negatively regulated each other in cultured osteoblastic cells. In this study, however, cancellation of the negative effects of IL-6/sIL-6R on osteoblast differentiation by inhibitors was incomplete as compared to the absence of inhibitor (Figs. 5, 6). This might be because ERK, Akt and

STAT3 are all critical pathways in osteoblast differentiation even in the absence of IL-6/sIL-6R, and even though one pathway is blocked, another pathway is enhanced by reciprocal regulation in the crosstalk between IL-6-activated signaling pathways (Fig. 9). Our results demonstrated that a STAT3 inhibitor significantly enhanced IL-6-induced activation of ERK and SHP2, but not of Akt (Fig. 4a). SHP2 could predominantly lead to the activation of the ERK signaling pathway as compared to Akt, and the enhanced signaling of ERK may restrain the enhancement of the Akt signaling pathway in a negative feedback manner.

The results obtained from the present study show that SHP2, MEK and PI3K inhibitors would be of potential use for the treatment of osteoporotic changes in RA patients. In particular, SHP2 inhibitors not only could inhibit the negative effect of IL-6-induced MEK/ERK and PI3K/Akt2 signaling, but also enhance the positive effect of IL-6-induced STAT3 signaling on osteoblast differentiation [37]. However, since a pro-inflammatory effect of STAT3 on synovitis has been reported [36, 58], selective inhibition of MEK2 and Akt2 signaling in osteoblasts may be more promising in order to avoid the enhancement of synovitis and consequent joint destruction.

In conclusion, our study provides new insights in the pathophysiology as well as potential treatment options for bone loss in RA, focusing on osteoblast differentiation in vitro. Our results demonstrated that IL-6 could inhibit osteoblast differentiation through MEK2/ERK and PI3K/Akt2 signaling pathways, both of which are SHP2-dependent downstream signaling pathways.

Conflict of interest All authors have no conflicts of interest.

References

1. Hashizume M, Mihara M (2011) The roles of interleukin-6 in the pathogenesis of rheumatoid arthritis. *Arthritis* 2011:765624
2. Ito A, Itoh Y, Sasaguri Y, Morimatsu M, Mori Y (1992) Effects of interleukin-6 on the metabolism of connective tissue components in rheumatoid synovial fibroblasts. *Arthritis Rheum* 35:1197–1201
3. Nishimoto N, Kishimoto T (2004) Inhibition of IL-6 for the treatment of inflammatory diseases. *Curr Opin Pharmacol* 4:386–391
4. De Benedetti F, Robbioni P, Massa M, Viola S, Albani S, Martini A (1992) Serum interleukin-6 levels and joint involvement in polyarticular and pauciarticular juvenile chronic arthritis. *Clin Exp Rheumatol* 10:493–498
5. De Benedetti F, Massa M, Pignatti P, Albani S, Novick D, Martini A (1994) Serum soluble interleukin 6 (IL-6) receptor and IL-6/soluble IL-6 receptor complex in systemic juvenile rheumatoid arthritis. *J Clin Invest* 93:2114–2119
6. Kotake S, Sato K, Kim KJ, Takahashi N, Udagawa N, Nakamura I, Yamaguchi A, Kishimoto T, Suda T, Kashiwazaki S (1996) Interleukin-6 and soluble interleukin-6 receptors in the synovial fluids from rheumatoid arthritis patients are responsible for osteoclast-like cell formation. *J Bone Miner Res* 11:88–95
7. Kwan Tat S, Padrines M, Theoleyre S, Heymann D, Fortun Y (2004) IL-6, RANKL, TNF-alpha/IL-1: interrelations in bone resorption pathophysiology. *Cytokine Growth Factor Rev* 15:49–60
8. Palmqvist P, Persson E, Conaway HH, Lerner UH (2002) IL-6, leukemia inhibitory factor, and oncostatin M stimulate bone resorption and regulate the expression of receptor activator of NF-kappa B ligand, osteoprotegerin, and receptor activator of NF-kappa B in mouse calvariae. *J Immunol* 169:3353–3362
9. Le Goff B, Blanchard F, Berthelot JM, Heymann D, Maugars Y (2010) Role for interleukin-6 in structural joint damage and systemic bone loss in rheumatoid arthritis. *Joint Bone Spine* 77:201–205
10. Hirano T, Matsuda T, Turner M, Miyasaka N, Buchan G, Tang B, Sato K, Shimizu M, Maini R, Feldmann M et al (1988) Excessive production of interleukin 6/B cell stimulatory factor-2 in rheumatoid arthritis. *Eur J Immunol* 18:1797–1801
11. Ohshima S, Saeki Y, Mima T, Sasai M, Nishioka K, Nomura S, Kopf M, Katada Y, Tanaka T, Suemura M, Kishimoto T (1998) Interleukin 6 plays a key role in the development of antigen-induced arthritis. *Proc Natl Acad Sci USA* 95:8222–8226
12. Dasgupta B, Corkill M, Kirkham B, Gibson T, Panayi G (1992) Serial estimation of interleukin 6 as a measure of systemic disease in rheumatoid arthritis. *J Rheumatol* 19:22–25
13. Poli V, Balena R, Fattori E, Markatos A, Yamamoto M, Tanaka H, Ciliberto G, Rodan GA, Costantini F (1994) Interleukin-6 deficient mice are protected from bone loss caused by estrogen depletion. *EMBO J* 13:1189–1196
14. Yang X, Ricciardi BF, Hernandez-Soria A, Shi Y, Pleshko Camacho N, Bostrom MP (2007) Callus mineralization and maturation are delayed during fracture healing in interleukin-6 knockout mice. *Bone* 41:928–936
15. Kopf M, Baumann H, Freer G, Freudenberg M, Lamers M, Kishimoto T, Zinkernagel R, Bluethmann H, Kohler G (1994) Impaired immune and acute-phase responses in interleukin-6-deficient mice. *Nature* 368:339–342
16. De Benedetti F, Rucci N, Del Fattore A, Peruzzi B, Paro R, Longo M, Vivarelli M, Muratori F, Berni S, Ballanti P, Ferrari S, Teti A (2006) Impaired skeletal development in interleukin-6-transgenic mice: a model for the impact of chronic inflammation on the growing skeletal system. *Arthritis Rheum* 54:3551–3563
17. Naka T, Nishimoto N, Kishimoto T (2002) The paradigm of IL-6: from basic science to medicine. *Arthritis Res* 4(Suppl 3):S233–S242
18. Wong PK, Campbell IK, Egan PJ, Ernst M, Wicks IP (2003) The role of the interleukin-6 family of cytokines in inflammatory arthritis and bone turnover. *Arthritis Rheum* 48:1177–1189
19. Garnero P, Thompson E, Woodworth T, Smolen JS (2010) Rapid and sustained improvement in bone and cartilage turnover markers with the anti-interleukin-6 receptor inhibitor tocilizumab plus methotrexate in rheumatoid arthritis patients with an inadequate response to methotrexate: results from a substudy of the multicenter double-blind, placebo-controlled trial of tocilizumab in inadequate responders to methotrexate alone. *Arthritis Rheum* 62:33–43
20. Franchimont N, Wertz S, Malaise M (2005) Interleukin-6: an osteotropic factor influencing bone formation? *Bone* 37:601–606
21. Li YP, Stashenko P (1992) Proinflammatory cytokines tumor necrosis factor-alpha and IL-6, but not IL-1, down-regulate the osteocalcin gene promoter. *J Immunol* 148:788–794
22. Peruzzi B, Cappariello A, Del Fattore A, Rucci N, De Benedetti F, Teti A (2012) c-Src and IL-6 inhibit osteoblast differentiation and integrate IGFBP5 signalling. *Nat Commun* 3:630
23. Hughes FJ, Howells GL (1993) Interleukin-6 inhibits bone formation in vitro. *Bone Miner* 21:21–28
24. Nishimura R, Moriyama K, Yasukawa K, Mundy GR, Yoneda T (1998) Combination of interleukin-6 and soluble interleukin-6 receptors induces differentiation and activation of JAK-STAT and MAP kinase pathways in MG-63 human osteoblastic cells. *J Bone Miner Res* 13:777–785
25. Taguchi Y, Yamamoto M, Yamate T, Lin SC, Mocharla H, DeTogni P, Nakayama N, Boyce BF, Abe E, Manolagas SC (1998) Interleukin-6-type cytokines stimulate mesenchymal progenitor differentiation toward the osteoblastic lineage. *Proc Assoc Am Physicians* 110:559–574
26. Ishihara K, Hirano T (2002) Molecular basis of the cell specificity of cytokine action. *Biochim Biophys Acta* 1592:281–296
27. Takahashi-Tezuka M, Yoshida Y, Fukada T, Ohtani T, Yamana Y, Nishida K, Nakajima K, Hibi M, Hirano T (1998) Gab1 acts as an adapter molecule linking the cytokine receptor gp130 to ERK mitogen-activated protein kinase. *Mol Cell Biol* 18:4109–4117
28. Hideshima T, Nakamura N, Chauhan D, Anderson KC (2001) Biologic sequelae of interleukin-6 induced PI3-K/Akt signaling in multiple myeloma. *Oncogene* 20:5991–6000
29. Tu Y, Gardner A, Lichtenstein A (2000) The phosphatidylinositol 3-kinase/AKT kinase pathway in multiple myeloma plasma cells: roles in cytokine-dependent survival and proliferative responses. *Cancer Res* 60:6763–6770
30. Chung TD, Yu JJ, Kong TA, Spiotto MT, Lin JM (2000) Interleukin-6 activates phosphatidylinositol-3 kinase, which inhibits apoptosis in human prostate cancer cell lines. *Prostate* 42:1–7
31. Qiu Y, Robinson D, Pretlow TG, Kung HJ (1998) Etk/Bmx, a tyrosine kinase with a pleckstrin-homology domain, is an effector of phosphatidylinositol 3'-kinase and is involved in interleukin 6-induced neuroendocrine differentiation of prostate cancer cells. *Proc Natl Acad Sci USA* 95:3644–3649
32. Chen RH, Chang MC, Su YH, Tsai YT, Kuo ML (1999) Interleukin-6 inhibits transforming growth factor-beta-induced apoptosis through the phosphatidylinositol 3-kinase/Akt and signal transducers and activators of transcription 3 pathways. *J Biol Chem* 274:23013–23019
33. Schmidt K, Schinke T, Haberland M, Priemel M, Schilling AF, Muelndner C, Rueger JM, Sock E, Wegner M, Amling M (2005) The high mobility group transcription factor Sox8 is a negative regulator of osteoblast differentiation. *J Cell Biol* 168:899–910

34. Ratisoontorn C, Seto ML, Broughton KM, Cunningham ML (2005) In vitro differentiation profile of osteoblasts derived from patients with Saethre-Chotzen syndrome. *Bone* 36:627–634
35. Hellmuth K, Grosskopf S, Lum CT, Wurtele M, Roder N, von Kries JP, Rosario M, Rademann J, Birchmeier W (2008) Specific inhibitors of the protein tyrosine phosphatase Shp2 identified by high-throughput docking. *Proc Natl Acad Sci USA* 105:7275–7280
36. Ernst M, Inglese M, Waring P, Campbell IK, Bao S, Clay FJ, Alexander WS, Wicks IP, Tarlinton DM, Novak U, Heath JK, Dunn AR (2001) Defective gp130-mediated signal transducer and activator of transcription (STAT) signaling results in degenerative joint disease, gastrointestinal ulceration, and failure of uterine implantation. *J Exp Med* 194:189–203
37. Itoh S, Udagawa N, Takahashi N, Yoshitake F, Narita H, Ebisu S, Ishihara K (2006) A critical role for interleukin-6 family-mediated Stat3 activation in osteoblast differentiation and bone formation. *Bone* 39:505–512
38. Sims NA (2004) Glycoprotein 130 regulates bone turnover and bone size by distinct downstream signaling pathways. *J Clin Invest* 113:379–389
39. Kawamura N, Kugimiya F, Oshima Y, Ohba S, Ikeda T et al (2007) Akt1 in osteoblasts and osteoclasts controls bone remodeling. *PLoS One* 2:e1058
40. Chen WS, Xu PZ, Gottlob K, Chen ML, Sokol K, Shiyanova T, Roninson I, Weng W, Suzuki R, Tobe K, Kadowaki T, Hay N (2001) Growth retardation and increased apoptosis in mice with homozygous disruption of the Akt1 gene. *Genes Dev* 15:2203–2208
41. Yang ZZ, Tschopp O, Hemmings-Mieszczyk M, Feng J, Brodbeck D, Perentes E, Hemmings BA (2003) Protein kinase B alpha/Akt1 regulates placental development and fetal growth. *J Biol Chem* 278:32124–32131
42. Vandoorne K, Magland J, Plaks V, Sharir A, Zelzer E, Wehrli F, Hemmings BA, Harmelin A, Neeman M (2010) Bone vascularization and trabecular bone formation are mediated by PKB alpha/Akt1 in a gene-dosage-dependent manner: in vivo and ex vivo MRI. *Magn Reson Med* 64:54–64
43. Choi YH, Choi HJ, Lee KY, Oh JW (2012) Akt1 regulates phosphorylation and osteogenic activity of Dlx3. *Biochem Biophys Res Commun* 425:800–805
44. Mukherjee A, Rotwein P (2012) Selective signaling by Akt1 controls osteoblast differentiation and osteoblast-mediated osteoclast development. *Mol Cell Biol* 32:490–500
45. Mukherjee A, Wilson EM, Rotwein P (2010) Selective signaling by Akt2 promotes bone morphogenetic protein 2-mediated osteoblast differentiation. *Mol Cell Biol* 30:1018–1027
46. Ducy P, Desbois C, Boyce B, Pinero G, Story B, Dunstan C, Smith E, Bonadio J, Goldstein S, Gundberg C, Bradley A, Karsenty G (1996) Increased bone formation in osteocalcin-deficient mice. *Nature* 382:448–452
47. Higuchi C, Myoui A, Hashimoto N, Kuriyama K, Yoshioka K, Yoshikawa H, Itoh K (2002) Continuous inhibition of MAPK signaling promotes the early osteoblastic differentiation and mineralization of the extracellular matrix. *J Bone Miner Res* 17:1785–1794
48. Chaudhary LR, Avioli LV (2000) Extracellular-signal regulated kinase signaling pathway mediates downregulation of type I procollagen gene expression by FGF-2, PDGF-BB, and okadaic acid in osteoblastic cells. *J Cell Biochem* 76:354–359
49. Lin FH, Chang JB, Brigman BE (2011) Role of mitogen-activated protein kinase in osteoblast differentiation. *J Orthop Res* 29:204–210
50. Ge C, Xiao G, Jiang D, Franceschi RT (2007) Critical role of the extracellular signal-regulated kinase-MAPK pathway in osteoblast differentiation and skeletal development. *J Cell Biol* 176:709–718
51. Matsushita T, Chan YY, Kawanami A, Balmes G, Landreth GE, Murakami S (2009) Extracellular signal-regulated kinase 1 (ERK1) and ERK2 play essential roles in osteoblast differentiation and in supporting osteoclastogenesis. *Mol Cell Biol* 29:5843–5857
52. Schindeler A, Little DG (2006) Ras-MAPK signaling in osteogenic differentiation: friend or foe? *J Bone Miner Res* 21:1331–1338
53. Sims NA, Jenkins BJ, Quinn JM, Nakamura A, Glatt M, Gillespie MT, Ernst M, Martin TJ (2004) Glycoprotein 130 regulates bone turnover and bone size by distinct downstream signaling pathways. *J Clin Invest* 113:379–389
54. Duplomb L, Baud'huin M, Charrier C, Berreur M, Trichet V, Blanchard F, Heymann D (2008) Interleukin-6 inhibits receptor activator of nuclear factor kappaB ligand-induced osteoclastogenesis by diverting cells into the macrophage lineage: key role of Serine727 phosphorylation of signal transducer and activator of transcription 3. *Endocrinology* 149:3688–3697
55. Yamanaka Y, Nakajima K, Fukada T, Hibi M, Hirano T (1996) Differentiation and growth arrest signals are generated through the cytoplasmic region of gp130 that is essential for Stat3 activation. *EMBO J* 15:1557–1565
56. Nakajima K, Yamanaka Y, Nakae K, Kojima H, Ichiba M, Kiuchi N, Kitaoka T, Fukada T, Hibi M, Hirano T (1996) A central role for Stat3 in IL-6-induced regulation of growth and differentiation in M1 leukemia cells. *EMBO J* 15:3651–3658
57. Hirano T, Matsuda T, Nakajima K (1994) Signal transduction through gp130 that is shared among the receptors for the interleukin 6 related cytokine subfamily. *Stem Cells* 12:262–277
58. Krause A, Scaletta N, Ji JD, Ivashkiv LB (2002) Rheumatoid arthritis synoviocyte survival is dependent on Stat3. *J Immunol* 169:6610–6616



Original Full Length Article

Novel sandwich ELISAs for rat DMP1: Age-related decrease of circulatory DMP1 levels in male rats



Sunao Sato ^a, Jun Hashimoto ^b, Yu Usami ^c, Kaname Ohyama ^d, Yukihiro Isogai ^e, Yoshiaki Hagiwara ^f, Nobuhiro Maruyama ^f, Toshihisa Komori ^g, Tatsuhiro Kuroda ^e, Satoru Toyosawa ^{a,*}

^a Department of Oral Pathology, Graduate School of Dentistry, Osaka University, Osaka, Japan

^b Rheumatoid Center, National Hospital Organization, Osaka Minami Medical Center, Japan

^c Clinical Laboratory, Osaka University Dental Hospital, Osaka, Japan

^d Department of Environmental and Pharmaceutical Sciences, Graduate School of Biomedical Sciences, Nagasaki University, Nagasaki, Japan

^e Project for Bone Metabolic Diseases, Pharmaceuticals Sales Division, Asahi Kasei Pharma Corporation, Tokyo, Japan

^f Immuno-Biological Laboratories Co., Ltd, Gunma, Japan

^g Department of Developmental and Reconstructive Medicine, Nagasaki University Graduate School of Biomedical Sciences, Nagasaki, Japan

ARTICLE INFO

Article history:

Received 24 May 2013

Revised 14 September 2013

Accepted 20 September 2013

Available online 26 September 2013

Edited by: Toshio Matsumoto

Keywords:

Dentin matrix protein 1 (DMP1)

Enzyme-linked immunosorbent assay (ELISA)

Osteocyte

Bone turnover

Aging

ABSTRACT

Dentin matrix protein 1 (DMP1), a noncollagenous bone matrix protein produced by osteocytes, regulates matrix mineralization and phosphate homeostasis. The lack of a precise assay for circulating DMP1 levels impairs further investigation of the protein's biological significance. Because full-length precursor DMP1 is cleaved into NH₂- and COOH-terminal fragments during the secretory process, we developed two new sandwich ELISAs for the NH₂- and COOH-terminal fragments of rat DMP1. One of these ELISAs, ELISA 1–2, is based on two affinity-purified polyclonal antibodies against the DMP1-1 and DMP1-2 peptides of the NH₂-terminal fragment, whereas the other, ELISA 4–3, is based on two affinity-purified polyclonal antibodies against the DMP1-3 and DMP1-4 peptides of the COOH-terminal fragment. The polyclonal antibodies were characterized in immunohistochemical and liquid chromatography–electrospray ionization tandem mass spectrometry (LC–MS/MS) studies. Immunohistochemical analyses of rat bone using these polyclonal antibodies revealed DMP1 immunoreactivity in osteocytes and pericanalicular matrix, consistent with the previously reported osteocyte-specific expression of DMP1. LC–MS/MS analyses of rat plasma-derived immunoreactive products affinity-extracted with these antibodies revealed the presence of DMP1 in circulating blood. The ELISAs established with these antibodies met accepted standards for reproducibility, repeatability, precision, and accuracy. Circulating DMP1 and levels of other biochemical markers (osteocalcin, Trap5b, Dkk-1, and SOST) were measured in 2-, 4-, 8-, 12-, 18-, 24-, 72-, and 96-week-old Wistar male rats. Circulating DMP1 levels determined by ELISAs 1–2 and 4–3 significantly decreased with age. During rapid skeletal growth (2–12 weeks), DMP1 levels measured by ELISA 4–3 were over three times higher than those measured by ELISA 1–2; however, DMP1 levels in old animals (72 and 96 weeks) were almost the same when measured by either ELISA. DMP1 levels determined by both ELISAs were most highly positively correlated with the level of Dkk-1, second most highly correlated with the level of osteocalcin, and less highly correlated with the levels of Trap5b and SOST. These novel sandwich ELISAs for rat DMP1 are highly specific and allow precise measurements of circulating DMP1, which may be a new biochemical marker for osteocyte-mediated bone turnover.

© 2013 Elsevier Inc. All rights reserved.

Introduction

Dentin matrix protein 1 (DMP1), which is expressed in osteocytes [1], is a member of the SIBLING (Small Integrin-Binding Ligand, N-linked Glycoprotein) family of genetically related non-collagenous matrix proteins in mineralized tissues [2]. DMP1 contains an

unusually large number of acidic domains; because of its highly acidic nature, DMP1 can bind to calcium, thereby regulating matrix mineralization [3]. Protein chemistry analysis has shown that full-length DMP1 is synthesized as a precursor that is cleaved into NH₂-terminal 37-kDa and COOH-terminal 57-kDa fragments [4]; however, a full-length form (105 kDa) of DMP1 has also been detected in bone and dentin, albeit at considerably lower levels [5]. DMP1-null mice exhibit hypophosphatemia, leading to the discovery of DMP1 mutations associated with autosomal-recessive hypophosphatemic rickets (ARHR) in humans [6,7]. Both DMP1-null mice and individuals with ARHR exhibit elevated serum FGF23, which causes increased renal phosphate wasting

* Corresponding author at: Department of Oral Pathology, Graduate School of Dentistry, Osaka University, 1-8 Yamadaoka, Suita, Osaka 565-0871, Japan. Fax: +81 6 6879 289.

E-mail address: toyosawa@dent.osaka-u.ac.jp (S. Toyosawa).

leading to hypophosphatemia. These findings indicate that regulation of matrix mineralization by DMP1 is coupled to renal phosphate homeostasis via FGF23 production by osteocytes.

Cellular and extracellular components of the skeletal tissue have been used to develop the biochemical markers that specifically reflect either bone formation or bone resorption [8]. These markers may be classified according to the biological compartment to which they belong, parameters of cellular (osteoblast and osteoclast) activity, and components released during bone formation and breakdown of the bone matrix. Osteocytes, which are the most abundant and longest-living cells in the adult skeleton, have recently been found to control bone remodeling through regulation of both osteoclast and osteoblast activity, and also to function as endocrine cells [9]. The targeted ablation of osteocytes in cortical bone generated osteoclast activation [10]. On the other hands, osteocyte as a mechanosensory cells coordinates the osteoblastic activity to mechanical force by downregulating sclerostin [11]. Further, osteocyte as an endocrine cell produces FGF-23, which leads to phosphate excretion in the kidney, thereby controls circulation phosphate [6]. These findings indicated that osteocyte viability and activity clearly plays a significant role in the maintenance of bone homeostasis and integrity. In fact, osteocyte density was decreased in the vertebral fracture patients than in the controls [12], and osteocyte lacunar density was decreased with an increase in bony porosity and microcrack density [13]. Until now, these osteocytic changes have been studied with histomorphometric analysis and three-dimensional imaging analyses of bone samples [14]. However, these methods give information on limited areas of whole skeletal bone and are not the noninvasive techniques suitable for routine analyses. Given that DMP1 is produced predominantly in osteocytes, whereas other bone matrix proteins (including osteopontin, osteocalcin, and bone sialoprotein) are produced in osteoblasts [1,15–17], circulating DMP1 represents a candidate biochemical marker for osteocyte activity as well as bone mineralization.

To assess the potential utility of DMP1 as a biochemical marker of bone metabolism under physiological and pathological conditions, it would be very useful to develop precise assays for measurement of DMP1 levels in circulating blood, and to use these assays to evaluate the normal range of circulating DMP1 levels. In this study, we

quantitatively determined the normal range of circulating DMP1 levels in rats of various ages (2–96 weeks) using newly development sandwich ELISAs, and analyzed the relationship between the levels of DMP1 and other biochemical markers of bone metabolism.

Materials and methods

Production of polyclonal antibodies against rat DMP1

Peptides encoding rat DMP1 residues 90–111 (DMP1-1: SGDDTFG DEDNGPGPEERQWGG), 148–164 (DMP1-2: HHSDEADSRPEAGDSTQ), 247–261 (DMP1-3: FRRSRVSEEDDRGEL), and 275–293 (DMP1-4: EDFRSKEESRSETQEDTAE) were prepared, with cysteines affixed NH₂-terminally to DMP1-1, -3, and -4 and COOH-terminally to DMP1-2 (American Peptide Company, Sunnyvale, CA, USA) (Fig. 1). The cysteinyl peptides were conjugated to bovine thyroglobulin and dialyzed, and the coupled peptides were then mixed with Freund's complete adjuvant (DIFCO, Lawrence, KS, USA) and injected subcutaneously into two Japanese white rabbits (approximately 100 µg per animal). Eight subcutaneous booster injections with Freund's incomplete adjuvant (DIFCO) were also performed (approximately 100 µg per animal). Anti-rat DMP1 peptide antisera were affinity-purified by acetic acid elution from a peptide-conjugated Activated Thiol Sepharose4B (GE Healthcare Life Sciences, Pittsburgh, PA, USA). Affinity-purified rabbit polyclonal antibodies against rat DMP1 peptides were used for immunohistochemistry, immunoaffinity chromatography, and rat DMP1 ELISAs. All animal procedures in this study were approved by Osaka University Graduate School of Dentistry Intramural Animal Use and Care Committee.

Immunohistochemistry of rat bone

One-week-old Wistar rats ($n = 3$) were fixed by transcardiac perfusion of 4% paraformaldehyde under general anesthesia. Tibia samples were immersed in fixative overnight at 4 °C and demineralized with buffered 10% EDTA for 7 days at 4 °C. The samples were embedded in paraffin, and serial sections (5 µm thick) were prepared and mounted onto silane-coated slides.



Fig. 1. Amino-acid sequence of rat DMP1. The sequences of peptides DMP1-1, -2, -3, and -4, used for immunization, are shown with a shaded background and underlining. The DMP1 peptides identified by LC-MS/MS analyses of plasma-derived immunoreactive products affinity-purified with antibodies against DMP1-1 or DMP1-3 are shown in bold type. Arrowheads indicated the cleavage sites between the NH₂-terminal 37-kDa and COOH-terminal 57-kDa fragments [4].

Immunohistochemical staining was performed using the streptavidin-biotin complex (sABC) peroxidase method and the anti-rabbit sABC system from Dako (Glostrup, Denmark). Primary rabbit polyclonal antibodies against DMP1-1, -2, -3, and -4 were used. Tissue sections were treated with trypsin to facilitate antigen exposure for immunostaining. Sections were lightly counterstained with hematoxylin. As negative controls, rabbit serum IgG (Dako) was used as the primary antibody, yielding uniformly negative results.

Peptide sequencing of immunoreactive products with antibodies for DMP1

Each immunoreactive product was extracted from 20 mL EDTA plasma of 1-month-old male Wistar rats by immunoaffinity chromatography, using antibodies against the DMP1-1 or DMP1-3 peptides. The immunoreactive product was condensed by freeze-dehydration and used for peptide sequencing. Digestion of these products followed an established methodology [18]. Briefly, the products (approximately 200 ng/100 μ L) were reduced with dithiothreitol (Wako Pure Chemical, Osaka, Japan) and then alkylated with iodoacetamide (Wako Pure Chemical). Subsequently, the samples were digested with trypsin (Promega, Madison, MI, USA) overnight at 37 °C.

The resulting peptide mixture was analyzed on a liquid chromatography–electrospray ionization tandem mass spectrometer (LC-MS/MS) (LTQ XL; Thermo Fisher Scientific, Waltham, MA, USA) equipped with a custom nano-LC system consisting of a Shimadzu LC pump (Shimadzu, Kyoto, Japan) with LC flow splitter (Dionex, Idstein, Germany) and an HCT PAL autosampler (CTC Analytics, Zwingen, Germany). The sample was loaded onto a nano-precolumn (300 μ m i.d. \times 5.0 mm, L-C-18; Chemicals and Evaluation and Research Institute, Tokyo, Japan) in the injection loop and washed using 0.1% trifluoroacetic acid in 2% acetonitrile. Peptides were separated using a nano-HPLC column (75 μ m i.d. \times 15 cm, Acclaim PepMap100C18, 3 μ m, Dionex) and ion-sprayed into the MS at a spray voltage of 1.5 kV. The mass spectrometer was configured to acquire data by progressing from a full scan of the sample to three tandem MS scans of the three precursor masses (m/z 730.2 corresponding to YQNTSESESEER; m/z 1000.6 corresponding to SEESKGDHEPTSTQDSDSQDVEFSSR; m/z 746.7 corresponding to SKEESNSTGSTSSSEEDNHPK) (Fig. 1) as determined in real time by the Xcalibur® software (Thermo Fisher Scientific). The MS/MS spectra obtained from these precursor ions were searched against the rat subdatabase of the public non-redundant protein database of the International Protein Index, version 3.87, provided by The European Bioinformatics Institute.

Generation of recombinant rat DMP1

Glutathione-S-transferase (GST)-fused rat DMP1 was created by subcloning a fragment of the coding region of the rat DMP1 cDNA (excluding the signal peptide) in an *E. coli* expression system, described previously [1]. Purified recombinant rat DMP1 was kept at -20 °C prior to use.

Development of sandwich ELISA for the detection of rat DMP1

The sandwich ELISA system for the detection of rat DMP1 was constructed by Immuno-Biological Laboratories Co., Ltd. (Gunma, Japan). Four affinity-purified antibodies were immobilized on the 96-well microtiter-plate, and conjugated horseradish peroxidase (HRP) (Toyobo, Osaka, Japan) was used to test different combinations of capture and detection antibodies in sandwich ELISA. In the assay, 100 μ L of recombinant rat DMP1 or rat blood samples were used. The assay procedure was as follows. Microtiter plates (96 wells) were coated by addition of 100 μ L of 100 mmol/L carbonate buffer (pH 9.5) containing 1.0 μ g of purified antibody to each well, followed by incubation overnight at 4 °C. The plates were washed with PBS containing 0.05% Tween-20 (PBS-T), and then blocked overnight at 4 °C with 200 μ L

per well of 1% (w/v) bovine serum albumin (BSA) in PBS containing 0.05% NaN_3 . Following two washes with PBS-T, test samples and recombinant rat DMP1 (as a standard) were added in duplicate to the wells of the coated microtiter plate and incubated for 1 h at 37 °C. After four washes with PBS-T, 100 μ L of HRP-conjugated antibody was added to each well, and the samples were incubated for 30 min at 4 °C. The wells were washed five times with PBS-T, and then 100 μ L of tetramethyl benzidine solution (Immuno-Biological Laboratories) was added to each well as a substrate, followed by incubation in the dark for 30 min at room temperature. The reaction was terminated by addition of 100 μ L of 0.5 mol/L H_2SO_4 . Absorbance of the solution was measured at 450 nm using an ELISA reader (iMark; Bio-Rad Laboratories, CA, USA). Finally the concentrations of unknown samples were calculated based on the recombinant rat DMP1 standard curve.

ELISA validation

In order to assess the intra- and inter-assay precision for the ELISA, three quality control (QC) samples were established covering the high, middle, and low range of the standard curves. Intra-assay precision was determined by 24 repeated measurements of each QC sample in a single plate, and inter-assay precision was determined by assessing each QC sample across six different plates in quintuplicate wells. Moreover, to assess the recovery rate in blood, different concentrations of recombinant rat DMP1 were added to samples and measured, and the recovery rate was calculated based on the difference between the measured and theoretical concentrations. The sensitivity of this kit was determined based on the guidelines provided by the National Committee for Clinical Laboratory Standards (NCCLS) Evaluation Protocols.

Other biochemical markers of bone metabolism

Plasma osteocalcin, a marker of bone formation, was measured by ELISA using antibodies raised against the middle region of human osteocalcin (Rat-MID™ Osteocalcin EIA; Immunodiagnostic Systems, Fountain Hills, AZ, USA). Plasma tartrate-resistant acid phosphatase isoenzyme 5b (TRAP5b), an osteoclast-specific enzyme, was measured by ELISA using a capture antibody raised against recombinant mouse TRAP5b (RatTRAP™; Immunodiagnostic Systems). Plasma Dickkopf-1 (Dkk-1), an osteocyte-expressed soluble inhibitor of the Wnt signaling pathway, was measured by ELISA using a capture antibody raised against Dkk-1 (Dkk-1 [rat], EIA kit; Enzo Life Sciences, Farmingdale, NY, USA). Plasma sclerostin (SOST), an osteocyte-expressed negative regulator of bone formation, was measured by ELISA using a capture antibody raised against recombinant mouse SOST (Quantikine ELISA Mouse/Rat SOST Immunoassay; R&D Systems, Minneapolis, MN, USA).

Study subjects

For the determination of the levels of DMP1 and the other biochemical markers as a function of the age of the animal, blood samples (EDTA plasma) were collected from male Wistar rats at 2, 4, 8, 12, 18, 24, 72, and 96 weeks of age ($n = 43$).

Statistical analysis

All statistical analyses were performed using JMP (Japanese version 10.0.0, SAS Institute, Cary, NC, USA). All comparisons of results from different age groups were performed by ANOVA and subsequent Tukey–Kramer test. All bar diagrams represent mean values, and error bars represent standard deviations (SDs). The correlations were calculated using the Pearson correlation coefficient. Statistical significance was defined as $p < 0.05$.